

# Optimization of Active Suspension of a Vehicle with Limited Acting Forces

Jardel Soares Pinto, Sérgio Junichi Idehara

**Abstract**— Suspension is an essential component in vehicle design, whether it is used as a passenger, utility or high-performance vehicle. The main objective of suspension is to provide the vehicle with stability and passenger comfort. This means reducing vibrations from the road or other sources, and preserving the vehicle body structure from the forces generated by vibrations. This study focuses on the active suspension system. The work evaluated the usability of this type of suspension in a passenger car through analysis of a complete vehicle model with seven degrees of freedom. In this case, an anti-windup proportional integral derivative (PID) controller was used. During the fine tuning of the PID controller, the determination of parameters was made by a genetic algorithm implemented in Matlab software. The results show that the active suspension system considerably reduces the oscillations in the bodywork, providing greater comfort for the passengers. The anti-windup constraint guarantees a limited actuator force and reasonable required power.

**Index Terms**— Active suspension, Genetic Algorithm, Optimization, PID controller, Vibration

## 1 INTRODUCTION

The vehicle suspension system provides internal comfort to the occupants of the cabin. This is defined as the feeling of well-being provided by the vehicle to the passengers, and relates to the noise and vibration level, in addition to the physical and psychological state of occupants [1]. The suspension system can be understood as a mechanism that directly connects the wheels to the chassis. The system absorbs shocks from damage and irregularities in the road and provides compensation for vehicle dynamics in suspension deflection. The suspension system also serves as a mechanical filter to isolate low frequency excitation mainly in the range of 4 to 8Hz, which is near a sensitivity of vibration frequency of the human body [2]. It plays an important role in the overall vehicle performance, with regards to stability (handling characteristics) and safety as it allows a distribution of reaction forces between the wheels and the ground, and influences the roll motion of the vehicle [3]. The types of suspension can be classified as passive, semi-active and active [4]. In the passive system, the elastic forces of the suspension are determined only by the displacement of the springs and damping forces from the dampers. In both the semi-active and active systems, they can receive energy from other sources, such as the vehicle engine. The control forces of an active suspension system affect the body movement in order to reduce vibrations from dynamic disturbances [5], improving vehicle manoeuvrability and drive quality. Guglielmino et al. [6] points out that the first active suspension system was introduced in the 1980s in Formula 1 cars. Since then, many studies have been carried out in this field and, despite their advantages over passive systems, control systems are restricted to only a few high value-added automobiles, some off-road vehicles and high-performance cars. The active suspension system uses controlled actuators, which continuously generate forces in the suspension

system. This makes it possible to modify the dynamic characteristics of the system in real time. Therefore, the active suspension overcomes the design limitations of traditional passive suspension performance [7]. As an example of an application, Yao et al. [3] have proposed the use of an active suspension system to control vehicle tilt during cornering. The controller was based on a predictive model that reduced the occupant's perception of the lateral acceleration and lateral load transfer ratio, improving the path tracking performance of the vehicle.

There are several traditional controllers applied to this area, such as PID, optimal and robust control, and Skyhook strategies. In recent years, different control techniques have been developed seeking better performance, such as a new methodology from Min, Li & Tong [4] that applied an adaptive fuzzy inverse optimal control in an electromagnetic actuator model. Fuzzy logic was used to determine nonlinear characteristics and Barrier Lyapunov functions to the system constraints. The authors showed the results based on a numerical simulation of a quarter-car model. Similarly, Zhang & Li [8] have suggested a design of optimal control from adaptive neural network techniques. The authors considered the nonlinear dynamic characteristics of the system, unmeasured variables and constrained states (displacement, velocity and electrical current) in numerical simulations to validate the suspension performance. In addition, Hao, Yamashita & Kobayashi [2] have suggested a new controller design based on interconnection and damping assignment passivity-based control. The authors' proposition transforms a nonlinear suspension system into a virtual linear system by energy shaping and damping injection. The maximum control force achieved in the simulations of a quarter-car model was 2,500N. Other forms of control strategies use the prediction of road surfaces. For instance, Theunissen et al. [9] used a model predictive control combined with a preview road profile, named explicit model predictive control (e-MPC), to reduce the computational load of control of a Sport Utility Vehicle (SUV) with hydraulic active suspension. The authors experimentally validated the system to attenuate frequency components below 4Hz, using a Skyhook controller.

As Tseng and Hrovat [10] have analysed, although an active

- Jardel Soares Pinto has automotive engineering degree in Federal University of Santa Catarina, Brazil. E-mail: jardelsoares100@hotmail.com
- Sérgio Junichi Idehara is currently professor in Federal University of Santa Catarina, Brazil. E-mail: sergio.idehara@ufsc.br

suspension offers significant improvement in comfort and handling, it would require higher energy consumption, more complexity in design, increased costs and additional weight, and greater requirements for an accurate operating system. In order to alleviate this, the use of an optimized control algorithm may reduce some energy consumption and required force (with the lighter mass of the controller), while maintaining the controller's performance. For example, Chen & Chen [11] applied a particle swarm optimization on a multi-performance model of an active suspension system of a full-car. The authors determined the parameters of a LQR matrix to reduce the amplitude of the control input and save energy from the actuators. The objective of this study is the optimization process of an active suspension model submitted to external excitations, through computer simulations performed in Matlab software. To limit the control force in the suspension system, an anti-windup proportional integral derivative (PID) controller is employed. The optimization of the controller gains is achieved through the Genetic Algorithm (GA) technique. In this study, vehicle stability was not considered in the model.

## 2 VEHICLE DYNAMICS

In the interests of a clearer definition, the sprung mass is related with all the mass above the spring, such as the chassis, passengers and subsystems (subframe, engine, steering etc), while the unsprung mass comprises all components between the spring and the ground. The concept of vehicle dynamics is the study of movements and forces in a vehicle and its parts. Such as vibrations of the chassis, suspension, engine, gearbox and steering system in response to efforts applied by the environment and driver commands (cornering, drive and braking conditions). In longitudinal dynamics, there are movements of sprung mass on the  $x$  axis and rotations around the  $y$  axis. They come from excitations in driving or braking forces. In vertical dynamics, there are movements in  $z$  axis and the rotations around the  $x$  and the  $y$  axis. The vehicle's sprung mass receives road excitations through the suspension system and generates movements of bounce (pure vertical movement), pitch and roll rotations. Finally, in lateral dynamics, the movement occurs in the  $y$  axis and rotation occurs around the  $z$  axis from the excitation of lateral forces and is responsible for the vehicle cornering [12]. In this study, vehicle dynamics of interest is in the vertical degree of freedom and suspension system influence on sprung mass vibration, which represents passenger comfort. According to Cieslak et al. [13], the primary point with regard to vehicle comfort is about the user's experience, i.e., human perception. Indeed, the researcher [12] explained that one of the main criteria used by people to judge the quality of a vehicle is their perception of internal vibrations.

### 2.1 Suspension System

The sources of the vehicle excitation in vibration problem are from the road or from internal sources such as engine, wheels, transmission etc. Additionally, as cited by Hou, Cao & Zhan [14], the main objectives for the suspension system can be seen to improve passenger ride comfort and provide better grip conditions on the ground and tire contact through suspension de-

flexion. Savaresi et al. [15] points out that a conventional passive suspension consists of three main elements: an elastic element (generally a helical spring, but there are also pneumatic and leaf springs), which stores energy and provides a force opposite and proportional to the extension of the suspension, aiming to carry elastic force. Furthermore, a damping element (usually a hydraulic or pneumatic damper) provides an opposing dissipative force and is proportional to the suspension extension velocity. The last is the sprung and unsprung mass of the vehicle. Jiregna & Sirata [16] have explained that the passive suspension has a good relationship between cost and satisfaction in both the comfort and safety criteria, since they are simple, low cost and reliable, making this type of suspension extensively used in the automotive industry. However, an active suspension system designed for a better relationship between the ride comfort and road holding needs to improve vehicle performance.

The active suspension system may store, dissipate or introduce energy through actuators, controlled by algorithms and sensors. Hyniova [17] explains that this mechanism needs an external energy source to deliver energy to actuators, allowing them to control the system. The author considers it one of the biggest disadvantages of the system. Different types of actuators can be used, e.g., hydraulic, pneumatic and electromagnetic. Strassberger and Guldner [18] have reported that BMW developed an active suspension system based on a hydraulic system, called dynamic drive. This reduced the roll angle during cornering by placing a hydraulic rotary actuator in the centre of the rear anti-roll bar. However, the unsprung mass may increase due to the hydraulic actuator and pressured fluid. Conversely, Ho, Tran & Ahn [19] developed a pneumatic active suspension with adaptive sliding mode control applied to a test bench of the quarter-car. This would be a lighter solution than the hydraulic active suspension. A pneumatic spring, as variable stiffness with hysteresis, was controlled based on a nonlinear disturbance observer to include uncertain parameters, like the sprung mass value. The authors found a reduction of about 40% in acceleration compared with passive suspension. For hydraulic or pneumatic active suspensions, energy is supplied through a pump or compressor, and is usually driven by the vehicle's engine. An electric motor is used for electromagnetic suspension to control the forces between sprung and unsprung mass. For this last case, Sun, Wu, Yin & Wang [20] employed a linear electric motor as the active suspension actuator. A sky-hook controller was used for two degrees of freedom in an experimental test in order to evaluate the performance of the vibration attenuation. The work achieved improved performance in body acceleration and suspension deflection. In general, those solutions are suitable for applications with low bandwidth [21]. In electromagnetic active suspension, there are some advantages over the hydraulic or pneumatic system, such as the possibility of high bandwidth operation, better dynamic behaviour, greater efficiency, better stability, ease of control, an absence of fluids and more precise control of forces. Another advantage of the electromagnetic active suspension is the possibility of operating as a generator, which allows energy to be recovered when the actuator produces the damping force, reduc-

ing energy consumption. In this kind of active suspension, energy accounts for about one third of the power of a vehicle's air conditioning system [21] [22].

### 3 MATERIAL AND METHODS

The 1/4 vehicle model is illustrated in Fig. 1a, where the vertical displacement of the unsprung mass ( $z_{un}$ ) and the sprung mass is represented in the  $z$ -axis ( $z_s$ ). The vehicle movement (Fig. 1b) features bounce ( $z$ ) in vertical direction, rotation around the  $x$ -axis ( $\phi$ ) as the roll angle, and rotation around  $y$ -axis ( $\theta$ ) as the pitch angle. The PID controller employs a model of quarter vehicle (Fig. 1a) and it is applied to the full vehicle model with 7 dof (Fig. 1b), which has four controllers, one for each wheel. The purpose of the PID controller is to control the position of the sprung mass (bodywork), compared to the reference value (equilibrium position).

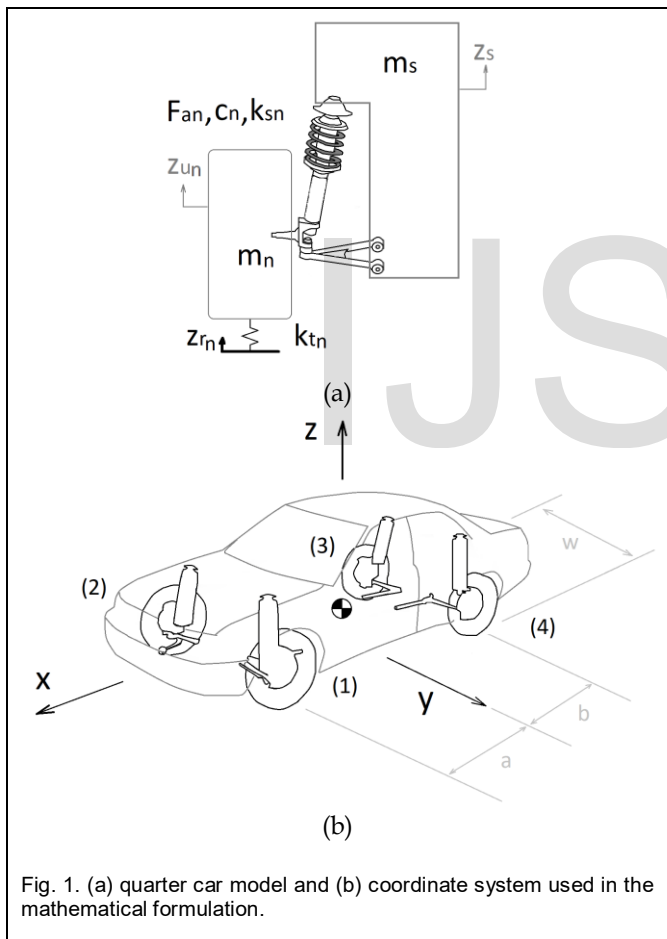


Fig. 1. (a) quarter car model and (b) coordinate system used in the mathematical formulation.

In this numerical model, the parameters are suspension stiffness ( $k_{sn}$ ), tire stiffness ( $k_{tn}$ ), suspension damping coefficient ( $C_n$ ), sprung mass ( $m_s$ ), unsprung mass ( $m_n$ ) and the variables  $z_s$ ,  $z_{un}$  and  $z_{rn}$  represent vertical displacements of the sprung mass, unsprung mass and the road profile, respectively.  $n$  is an integer value from one to four representing the set of 1/4 of the vehicle. The active force in each wheel is represented by  $F_{an}$ . The vehicle moment of inertia is  $I_{xx}$  and  $I_{yy}$ , the longitudinal distance from the suspension fixation to the centre of gravity

(CG) represented by  $a$  (front axle) and  $b$  (rear axle), and the vehicle track width  $w$ . The equation for this model is obtained by applying classic mechanics laws to describe the vertical motion of the vehicle and suspension fixations. The linearized equations for the unsprung mass dynamics are presented as follows:

$$k_{s1}(z_{s1} - z_{u1}) + C_1(\dot{z}_{s1} - \dot{z}_{u1}) - k_{t1}(z_{u1} - z_{r1}) + F_{a1} = m_1 \cdot \ddot{z}_{u1} \tag{1}$$

$$k_{s2}(z_{s2} - z_{u2}) + C_2(\dot{z}_{s2} - \dot{z}_{u2}) - k_{t2}(z_{u2} - z_{r2}) + F_{a2} = m_2 \cdot \ddot{z}_{u2} \tag{2}$$

$$k_{s3}(z_{s3} - z_{u3}) + C_3(\dot{z}_{s3} - \dot{z}_{u3}) - k_{t3}(z_{u3} - z_{r3}) + F_{a3} = m_3 \cdot \ddot{z}_{u3} \tag{3}$$

$$k_{s4}(z_{s4} - z_{u4}) + C_4(\dot{z}_{s4} - \dot{z}_{u4}) - k_{t4}(z_{u4} - z_{r4}) + F_{a4} = m_4 \cdot \ddot{z}_{u4} \tag{4}$$

Equation (5) represents the movement of the sprung mass measured from the centre of gravity.

$$-k_{s1}(z_{s1} - z_{u1}) - C_1(\dot{z}_{s1} - \dot{z}_{u1}) - k_{s2}(z_{s2} - z_{u2}) - C_2(\dot{z}_{s2} - \dot{z}_{u2}) - k_{s3}(z_{s3} - z_{u3}) - C_3(\dot{z}_{s3} - \dot{z}_{u3}) - k_{s4}(z_{s4} - z_{u4}) - C_4(\dot{z}_{s4} - \dot{z}_{u4}) - F_{a1} - F_{a2} - F_{a3} - F_{a4} = m_s \cdot \ddot{z}_s \tag{5}$$

For the angular displacement in  $x$  and  $y$  directions, the (6) and (7) are used.

$$\frac{w}{2} \cdot [-k_{s1}(z_{s1} - z_{u1}) - C_1(\dot{z}_{s1} - \dot{z}_{u1}) - F_{a1} - k_{s4}(z_{s4} - z_{u4}) - C_4(\dot{z}_{s4} - \dot{z}_{u4}) - F_{a4}] + \frac{w}{2} \cdot [k_{s2}(z_{s2} - z_{u2}) + C_2(\dot{z}_{s2} - \dot{z}_{u2}) + F_{a2} + k_{s3}(z_{s3} - z_{u3}) + C_3(\dot{z}_{s3} - \dot{z}_{u3}) + F_{a3}] = I_{xx} \ddot{\theta} \tag{6}$$

$$a[k_{s1}(z_{s1} - z_{u1}) + C_1(\dot{z}_{s1} - \dot{z}_{u1}) + F_{a1} + k_{s2}(z_{s2} - z_{u2}) + C_2(\dot{z}_{s2} - \dot{z}_{u2}) + F_{a2}] + b[-k_{s3}(z_{s3} - z_{u3}) - C_3(\dot{z}_{s3} - \dot{z}_{u3}) - F_{a3} - k_{s4}(z_{s4} - z_{u4}) - C_4(\dot{z}_{s4} - \dot{z}_{u4}) - F_{a4}] = I_{yy} \ddot{\theta} \tag{7}$$

The displacements ( $z_{s1}$ ,  $z_{s2}$ ,  $z_{s3}$  and  $z_{s4}$ ) and velocities ( $\dot{z}_{s1}$ ,  $\dot{z}_{s2}$ ,  $\dot{z}_{s3}$  and  $\dot{z}_{s4}$ ) at each point of the suspension fixation are obtained by:

$$z_{s1} = z_s - \theta \cdot a + \phi \cdot \frac{w}{2} \tag{8}$$

$$z_{s2} = z_s - \theta \cdot a - \phi \cdot \frac{w}{2} \tag{9}$$

$$z_{s3} = z_s + \theta \cdot b - \phi \cdot \frac{w}{2} \tag{10}$$

$$z_{s4} = z_s + \theta \cdot b + \phi \cdot \frac{w}{2} \tag{11}$$

$$\dot{z}_{s1} = \dot{z}_s - \dot{\theta} \cdot a + \dot{\phi} \cdot \frac{w}{2} \tag{12}$$

$$\dot{z}_{s2} = \dot{z}_s - \dot{\theta} \cdot a - \dot{\phi} \cdot \frac{w}{2} \tag{13}$$

$$\dot{z}_{s3} = \dot{z}_s + \dot{\theta} \cdot b - \dot{\phi} \cdot \frac{w}{2} \tag{14}$$

$$\dot{z}_{s4} = \dot{z}_s + \dot{\theta} \cdot b + \dot{\phi} \cdot \frac{w}{2} \tag{15}$$

**3.1 Vehicle Data**

The applied vehicle parameters in the simulation are from [23] and presented in Table 1, where the authors evaluated the suspension of a passenger car. This vehicle has a front suspension system with independent wheels, McPherson type, with helical springs and double-acting telescopic hydraulic shock absorbers. The rear suspension system is a lower double wishbone type and features independent wheels.

TABLE 1  
DATA OF THE VEHICLE MODEL

Parameter	Variable	Value
Total weight	-	830.0 kg
Sprung mass	$m_s$	678.0 kg
Frontal unsprung mass	$m_1, m_2$	31.5 kg
Rear unsprung mass	$m_3, m_4$	44.5 kg
Tire stiffness	$k_t$	190,000.0 N/m
Frontal spring stiffness	$k_{s1}$	16,879.3 N/m
Rear spring stiffness	$k_{s2}$	19,000.0 N/m
Frontal damping coefficient	$C_1$	1,554.0 Ns/m
Rear damping coefficient	$C_2$	3,144.2 Ns/m
Tire damping coefficient	$C_p$	0.0
Half track	$w_1, w_2$	0.6685 m
Distance between front wheel and CG	$a$	0.8820 m
Distance between rear wheel and CG	$b$	1.4795 m
Longitudinal mass moment of inertia	$I_{xx}$	2,353.5 kg.m <sup>2</sup>
Transversal mass moment of inertia	$I_{yy}$	850.0 kg.m <sup>2</sup>
Vehicle velocity	$v$	30.0 km/h

**3.2 Road Excitation Model**

The road pavement is considered rough with potholes, cracks and bumps randomly distributed. Therefore, the behavior of the suspension model for an excitation of a random road profile is evaluated numerically. A model for random road profiles was proposed by Ulsoy, Peng and Çakmakci [24], considering that the profile of the road surface is stochastic in nature and it can be represented by its statistical properties. A useful and compact representation of this profile is by the power spectral

density (PSD) from the road profile time signal. This calculation is made using a Fourier transform on the autocorrelation function. PSD of a random road profile,  $S_r$ , is expressed by Equation (16).

$$S_r(f') = S_0 \left| \frac{1/(f'^2)}{1 + (f'_0/f')^2} \right| \tag{16}$$

$$f' = \frac{f}{v} \tag{17}$$

$$f'_0 = \frac{f_c}{v} \tag{18}$$

$f'$  corresponds to spatial frequency, which represents the ratio between the excitation frequency ( $f$ ) and vehicle speed ( $v$ ), as shown by (17).  $S_0$  is the magnitude of roughness of the road, and it has a value of  $S_0 = 1.2510^{-3}$ ,  $f'_0$  is the spatial cut-off frequency and is expressed by (18). The ratio of cutoff frequency ( $f_c$ ) was  $f_c = 1.031 \text{ rad/m}$ .

**3.3 Anti-Windup PID Controller**

Industrial processes in practice are subject to some type of restriction in their control system. For example, force amplitude limitation, which may cause a decline in the performance of the controlled system. This limitation causes a phenomenon called windup. In the structure of the PID controller, when there is saturation in the actuator force, the control performance is deteriorated with larger overshoot, slower settling time and instability [25]. Therefore, the integral term of the PID controller reaches high values without causing any effect on the output plant, in the event that the integration error continues. In order to restore the integral term to steady state, the error must have a negative sign over a long interval time, causing a high overshoot and a long settling time. In view of this, an anti-windup method is implemented in the PID controller so that the system can perform without losing the control quality when saturating the active force. For the purposes of this study, the anti-windup algorithm is a linear technique called back calculation. Fig. 2 shows the control scheme. That structure is based on a classic PID controller that employs proportional ( $K$ ), derivative ( $K_d = K \cdot T_d$ ) and integral ( $K_i = K/T_i$ ) terms to obtain the amplitude of the control force. The parameters  $T_i$  and  $T_d$  are integral and derivative time constants. The controller input signal is the vertical displacement of the suspension fixation ( $z_{sn}$ ) on the sprung mass and the reference signal ( $r$ ) is the position of the static equilibrium.

In this method, when there is saturation at the output actuator, the integral term is recalculated so that its value remains below the actuator's limit. This correction is done dynamically with a time constant  $T_t$ .

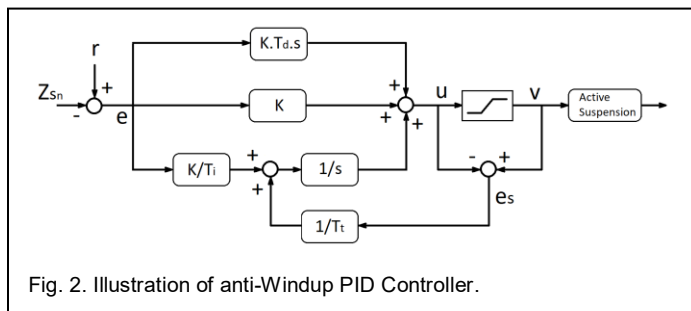


Fig. 2. Illustration of anti-Windup PID Controller.

The system has an additional feedback loop, where the difference between the actual controller force ( $u$ ) and the saturated controller force ( $v$ ) of the actuator constitutes an error  $e_s$ . The error value is fed back to the input of the integration with a gain value of  $K_b = 1/T_t$ . When there is no saturation, the  $e_s$  error is equal to zero. Thus, the additional loop will have no effect on the system when the controller is operating in a linear region (not saturated).

The feedback signal ( $h(t)$ ) at a given time of  $t$  is shown in Equation (19).

$$h(t) = K_b \cdot (v(t) - u(t)) \tag{19}$$

The gain  $K_b$  determines how much is subtracted from the portion to be integrated. The reduction in the integral term causes the control signal to leave the saturation region faster, reaching the steady-state value in a shorter time and improving the system's performance.

#### 4 GENETIC ALGORITHM (GA)

The Ziegler-Nichols tuning method allows us to solve several parameter adjustment problems facing the PID controller ( $K_p$ ,  $K_i$  and  $K_d$ ) in a relatively simple way in order to select the control parameters. However, the adjustment of the control parameters is not always accurate. Therefore, for this study, a Genetic Algorithm (GA) method was used to obtain the PID control parameters applied to the anti-windup technique. The Genetic Algorithm is a meta-heuristic search strategy for a given numerical problem and it can be used to optimize parameters of vehicle dynamics as indicated by Alkhatib, Jazar & Golnaragui [26]. The methodology allows us to thoroughly explore the space of viable solutions of the problem. GA is inspired by the biological dynamics of populations, which method searches for the best solution from a set of random initial solutions. New solutions are generated based on the population offspring and mutation process along several generations. The algorithm tries to avoid confinement in local minima or maxima locus and seeks for the global optimum.

At the initiation of GA, a random population is evaluated to determine the quality of the solution from fitness function. The best individuals from that population are selected to generate offspring through recombination/reproduction and mutation. During recombination or reproduction, new individuals are created by combining the genetic characteristics of their parents, while in mutation, a new individual is created by modifying one bit of the chromosome information, so that there is a genetic variety in the population. During the iterations of this generation, part of the original population is replaced by a new one, which is formed by crossing selected individuals from the previous population. The Table 2 shows the main parameters used in the optimization process by GA.

##### 4.1 GA optimization function

The objective is to reduce the vibrations of the vehicle body. In order to achieve this, GA aimed to search for the optimal parameters of the controller that reduces the sprung mass acceleration and displacement. An integration of the acceleration and displacement signals along time  $T$ , as presented in (20), was em-

ployed to determine the fitness value. The optimization algorithm seeks for maximum function solutions i.e., the minimization of the average vibration of the vehicle center of mass. The  $z_s$  is the sprung mass displacement measured from its center of gravity,  $T$  is the total time of the simulation and  $i$  is the GA individual (chromosome) identification. The vehicle model is subjected to an excitation on the tires based on the random PSD signal from (16): see the illustration in Fig. 3. The profiles are different for the left and right sides of the vehicle in order to simulate real driving conditions and on a very irregular road as a critical condition. This situation serves to assess the ability of the controller to attenuate the vibration generated by this road profile, consequently reaching a comfort feeling for the occupants. Fig. 4 shows a schematic illustration of the optimization process based on the complete model of the vehicle. The fitness of the initial population is calculated from the seven dof car model, and the GA identifies which individuals have higher fitness. The selection process filters the best solutions (parents) and makes new individuals (offspring) by crossing between the parents. For those new children, a new level of fitness is calculated and the sequence for the next generation restarts from the selection point. The search parameters are the PID control constants: proportional  $K_p$ , derivative  $K_d$ , integral  $K_i$  and anti-windup parameter  $K_b$ .

$$f_i = \frac{1}{T \int_0^T \ddot{z}_{s_i} \cdot dt} + \frac{1}{T \int_0^T z_{s_i} \cdot dt} \tag{20}$$

$$x^* = \underset{x \in S}{\operatorname{argmin}} (f_i) \tag{21}$$

Where, the parameter vector  $x = \{K_p \ K_i \ K_d \ K_b\}^T$  and  $S$  is the domain of the feasible region of the solutions.

TABLE 2  
GENETIC ALGORITHM PARAMETERS

Parameter	Value
Population size	50
Selection type	Roulette wheel selection
Crossover Type	Two points
Crossover Rate	0.80
Mutation type	Uniform
Mutation rate	5%
Number of generations	15
Search intervals	$K_p: [1 \cdot 10^3, 1 \cdot 10^7]$
	$K_i: [1 \cdot 10^3, 1 \cdot 10^7]$
	$K_d: [1 \cdot 10^3, 1 \cdot 10^7]$
	$K_b: [1, 200]$

## 5 RESULTS

### 5.1 Optimization result

The values of the controller gains obtained through the optimization by GA are shown in Table 3. Fig. 5 shows the GA's behavior over the iterations depending on the generations. This

graph represents the fitness level of each individual (represented by the asterisk). Two curves are observed, the dashed line representing the average of all individual solutions of each generation and the continuous line representing the best response of each generation. The optimal point obtained for this work (fitness value of 56.27) was achieved in six generations. Afterwards, the fitness of the individuals converged to the same value, decreasing the population standard deviation for each iteration. The first generation had an initial standard deviation of 7.3 and the last one of  $6.10^{-14}$ . As illustrated in Fig. 5, for this case, 15 generations were sufficient to obtain population convergence.

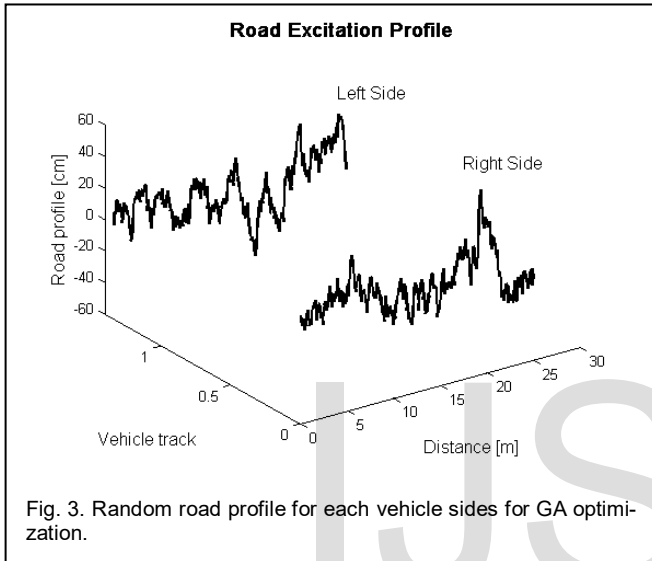


Fig. 3. Random road profile for each vehicle sides for GA optimization.

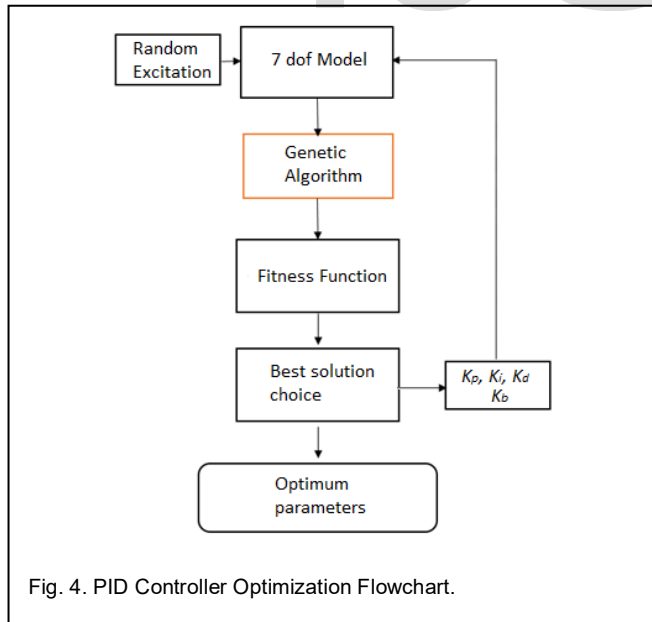


Fig. 4. PID Controller Optimization Flowchart.

With the values of the optimal control gains obtained in this optimization process, a numerical simulation of the complete model of the vehicle subjected to external random excitations was performed, solving the set of differential equations from

equation (1) to (7), and the results were compared with a traditional passive suspension response in the next section.

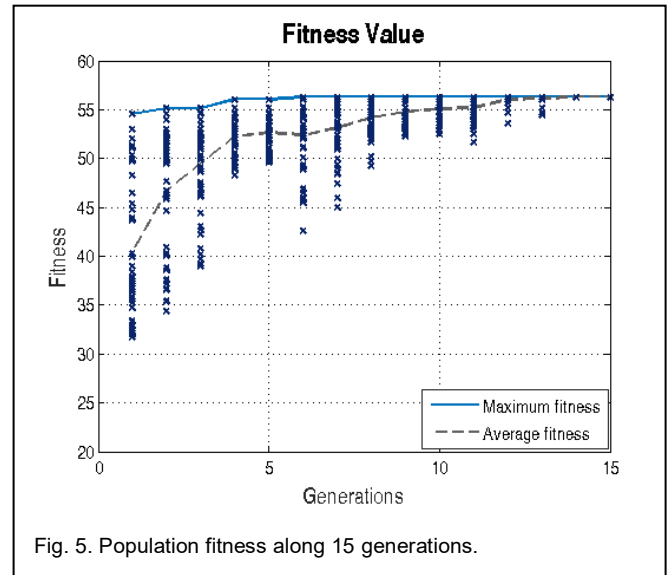


Fig. 5. Population fitness along 15 generations.

TABLE 3  
OPTIMIZED PID CONTROLLER GAINS WITH FORCE LIMITATION

PID controller gains	Value
$K_p$	$1.64 \cdot 10^6$
$K_i$	$1.20 \cdot 10^6$
$K_d$	$5.04 \cdot 10^4$
$K_b$	30.21

### 5.2 Optimized controller response

Fig. 6a shows the comparison between the passive suspension (gray) and optimized active suspension (black) of the sprung mass vertical displacement as a function of time when the model of the vehicle is excited by a random pathway. It can be seen from Fig. 6a that the controller of the active suspension system was able to attenuate the displacement of the vehicle body. This is noted around 17.5 s, where the displacement of the sprung mass was maximum for both suspensions. approximately 6.1 cm is for the passive system, and 0.4 cm is for active suspension. This amounts to a vibration reduction of 93.4% in relation to passive suspension. These results indicate an improvement in the passenger comfort for lower vibration amplitude. The simulation results for roll and pitch rotations are shown in Fig. 6b. For angular movements, the controllers also achieved considerable reductions in the displacement of the bodywork, by comparing the vibration peaks between active and passive suspension. There was a significant improvement in the vehicle dynamics, mainly with regards to roll motion. The maximum amplitude for the passive suspension was 4.4 degrees and 0.2 degrees in the controlled suspension, reducing the roll vibration by about 96.5%. For the pitch movement, the maximum amplitude of passive suspension was 0.9 degrees

and 0.2 degrees for active suspension, accumulating in a reduction of 77.4%. The lower oscillation in torsional degrees of freedom may enhance the vehicle stability characteristics, improving vehicle safety.

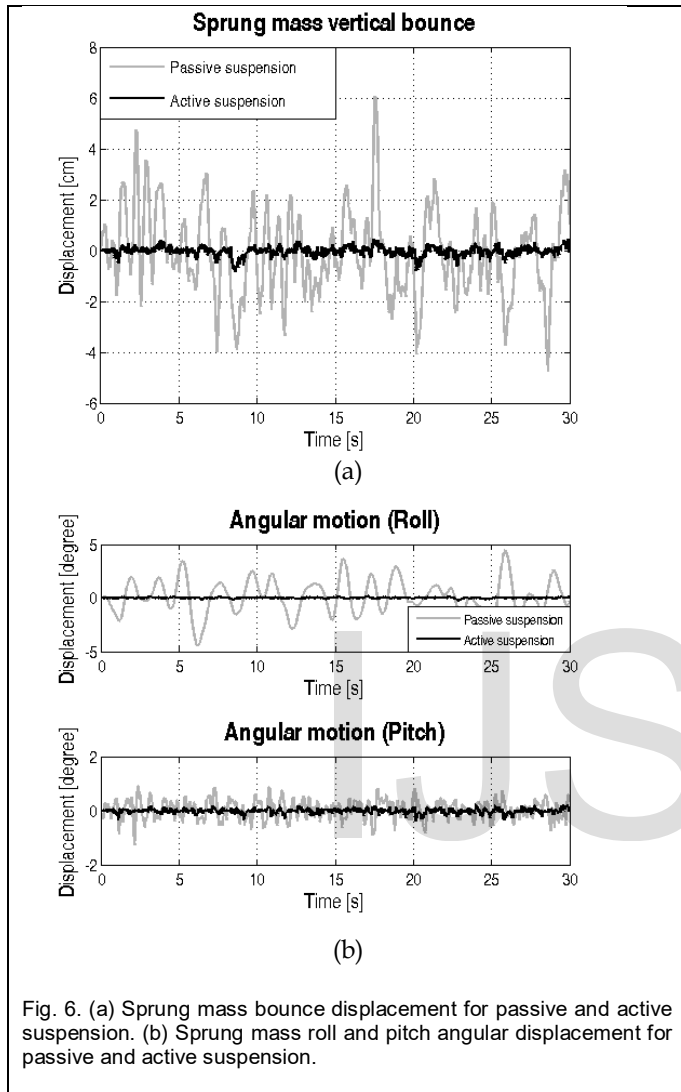


Fig. 6. (a) Sprung mass bounce displacement for passive and active suspension. (b) Sprung mass roll and pitch angular displacement for passive and active suspension.

Fig. 7a shows the applied control force for each suspension to result in the Fig. 6 response. As the controller is an anti-windup model with a force limitation of 5,000 N, the active forces do not exceed that limit. However, there are great irregularities in the road as represented in the simulation. The forces achieved that limit several times. Regarding the required power, the active suspension system enabled a limited use of power as illustrated in Fig. 7b. The maximum power required by each suspension was 267 W, 255 W, 830 W and 817 W, respectively, but for different time occurrences for points 1, 2, 3 and 4. Additionally, the maximum total power (sum of the powers of the four controllers) was 2,168 W (approximately 3 hp). It is noticeable that the random track profile imposes severe conditions for the PID controller to be able to act in the vibration reductions, since it needs to reduce large displacements in a short period of time, demanding higher power than a usual drive condition.

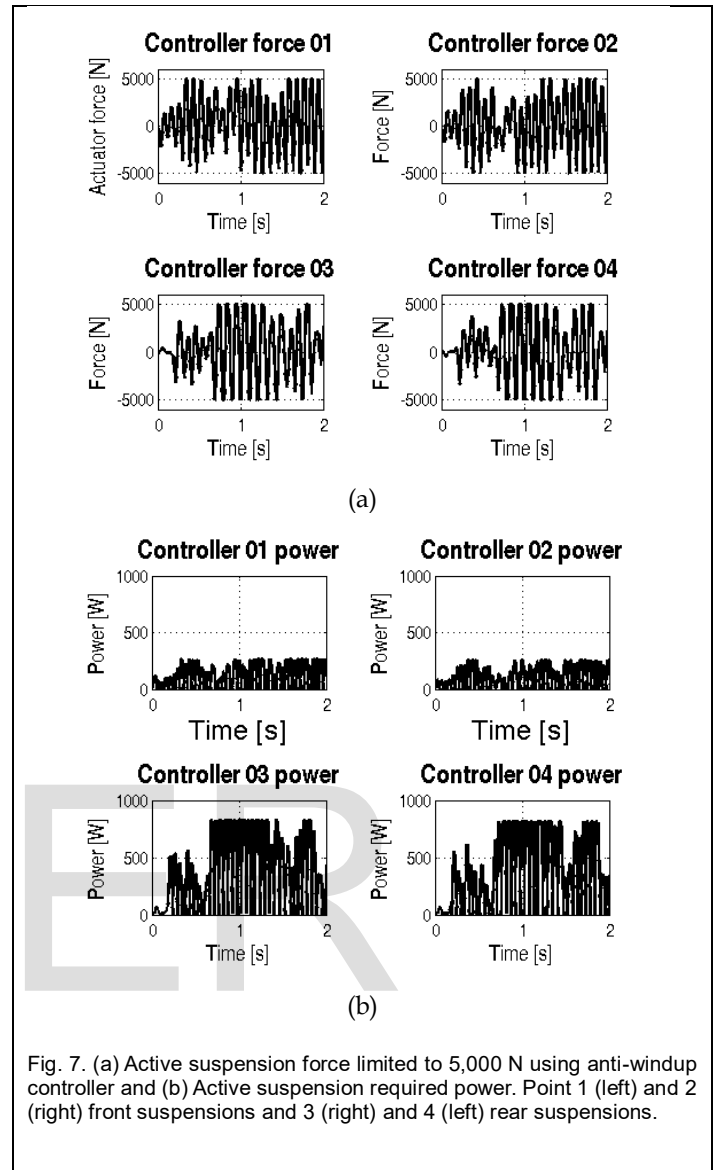


Fig. 7. (a) Active suspension force limited to 5,000 N using anti-windup controller and (b) Active suspension required power. Point 1 (left) and 2 (right) front suspensions and 3 (right) and 4 (left) rear suspensions.

## 6 CONCLUSION

In this study, the optimization of a PID controller applied to a vehicle active suspension system was carried out using genetic algorithm. The objective of this optimization was to improve the performance of the vehicle's suspension system in order to provide greater comfort to the passengers by reducing the oscillations coming from the road irregularities in the body of the vehicle. The use of controller gains obtained in the optimization process proved to be efficient in random types of excitations. Achieving an average reduction of 83.1% in the movements of the sprung mass compared to the passive system. The maximum force of each controller was set to 5,000 N, where the anti-windup PID controller could limit the actuating force without losing the quality of the vibration control. With the use of these optimized control parameters in the active suspension system, it needed a power peak of about 2,168 W to operate the four active suspensions in high excitation conditions. The advantage

of optimization applied to the active suspension system has been shown to have potential for automotive engineering in reducing vibrations, and providing greater comfort and safety to the vehicle occupants.

## REFERENCES

- [1]. J.Z. Xia et al., "Influence of Vehicle Suspension System on Ride Comfort," *Applied Mechanics and Materials*, vol. 141, no. 6, pp. 319-322, 2011.
- [2]. S. Hao, Y. Yamashita, K. Kobayashi, "Robust passivity-based control design for active nonlinear suspension system," *Int J Robust Nonlinear Control*, vol. 32, pp. 373-392, 2022.
- [3]. J. Yao, M. Wang, Z. Li, Y. Jia, "Research on Model Predictive Control for Automobile Active Tilt Based on Active Suspension," *Energies*, vol. 14, no. 671, pp. 1-18, 2021.
- [4]. X. Min, Y. Li, S. Tong, "Adaptive fuzzy optimal control for a class of active suspension systems with full-state constraints," *IET Intelligent Transport Systems*, vol. 14, no. 5, pp. 371-381, 2020.
- [5]. G. Genta, L. Morello, "The Automotive Chassis: Volume 1: Components Design," Dordrecht: Springer, 2009.
- [6]. E. Guglielmino, T. Sireteanu, C.W. Stammers, G. Ghita, M. Giuclea, "Semi-active Suspension Control: Improved Vehicle Ride and Road Friendliness," Springer-Verlag, 2008.
- [7]. J. Zhang, F. Ding, N. Zhang, S. Chen, B. Zhang, "A new SSUKF observer for sliding mode force tracking  $h^\infty$  control of electrohydraulic active suspension," *Asian Journal of Control*, vol. 22, no. 2, pp. 761-778, 2020.
- [8]. J. Zhang, Y. Li, "Neuro-adaptive output-feedback optimized stochastic control for the active suspension systems with state constraints," *Int J Adapt Control Signal Process*, vol. 36, pp. 38-68, 2022.
- [9]. J. Theunissen, A. Sorniotti, P. Gruber, S. Fallah, M. Ricco, M. Kvasnica, M. Dhaens, "Regionless explicit model predictive control of active suspension systems with preview," *IEEE Transactions on Industrial Electronics*, vol. 67, no. 6, pp. 4877-4888, 2020.
- [10]. E. H. Tseng, D. Hrovat, "State of the art survey: active and semi-active suspension Mobility," *Vehicle System Dynamics: International Journal of Vehicle Mechanics and Mobility*, vol. 53, no. 7, pp. 1034-1062, 2015.
- [11]. C.-C. Chen, Y.-T. Chen, "Global optimization control for nonlinear full-car active suspension system with multi-performances," *IET Control Theory & Applications*, vol. 15, pp. 1882-1905, 2021.
- [12]. T.D. Gillespie, "Fundamentals of Vehicle Dynamics," Warrendale: SAE International, 1992.
- [13]. M.P. Cieslak, S. Kanarachos, C. Diels, M. Blundell, A. Baxendale, M. Burnett, "Accurate ride comfort estimation combining accelerometer measurements, anthropometric data and neural networks," *Neural Computing and Applications*, vol. 32, no. 12, pp. 8747-8762, 2020.
- [14]. J. Hou, X. Cao, C. Zhan, "Symmetry control of comfortable vehicle suspension based on  $H^\infty$ ," *Symmetry*, vol. 14, no. 171, pp. 1-17, 2022.
- [15]. S.M. Savaresi et al., "Semi-Active Suspension Control Design for Vehicles," Burlington: Elsevier, 2010.
- [16]. I. Jiregna, G. Sirata, "A review of the vehicle suspension system," *Journal of Mechanical and Energy Engineering*, vol. 4, no. 2, pp. 109-114, 2020.
- [17]. K. Hyniova, "Energy control principles in an automotive active suspension system," *International Scientific Journal "Trans Motauto World"*, vol. 4, no. 3, pp. 107-110, 2019.
- [18]. M. Strassberger, J. Guldner, "BMW's dynamic drive: an active stabilizer bar system," *IEEE Control Systems Magazine*, vol. 24, no. 4, pp. 28-29, 2004.
- [19]. C.M. Ho, D.T. Tran, K.K. Ahn, "Adaptive sliding mode control based nonlinear disturbance observer for active suspension with pneumatic spring," *Journal of Sound and Vibration*, vol. 509, pp. 1-18, 2021.
- [20]. X. Sun, M. Wu, C. Yin, S. Wang, "Model predictive thrust force control for linear motor actuator used in active suspension," *IEEE Transactions on Energy Conversion*, vol. 36, no. 4, pp. 3063-3072, 2021.
- [21]. I. Martins et al., "Electromagnetic hybrid active-passive vehicle suspension system," In: 1999 IEEE 49th Vehicular Technology Conference, Houston, vol. 3, pp. 2273-2277, 1999.
- [22]. B.L.J. Gysen et al., "Active Electromagnetic Suspension System for Improved Vehicle Dynamics," *IEEE Transactions on Vehicular Technology*, vol. 59, no. 3, pp. 1156-1163, 2010.
- [23]. S.J. Idehara, M.R.R. Sabka, "Influence of model parameters on vehicle suspension control," *International Journal of Research in Engineering and Technology*, vol. 7, no. 12, pp. 1-11, 2018.
- [24]. A. G. Ulsoy, H. Peng, M. Çakmakci, "Automotive Control Systems," New York: Cambridge University, 2012.
- [25]. H.-B. Shin, J.-G. Park, "Anti-Windup PID controller with integral state predictor for variable-speed motor drives," *IEEE Transactions on Industrial Electronics*, vol. 59, no. 3, pp. 1509-1516, 2012.
- [26]. R. Alkhatib, G.N. Jazar, M.F. Golnaraghi, "Optimal design of passive linear suspension using genetic algorithm," *Journal of Sound and Vibration*, vol. 275, pp. 665-691, 2004.
- [27]. B.L.J. Gysen, "Generalized harmonic modeling technique for 2D electromagnetic problems," PhD thesis, Electrical Engineering, Technische Universiteit Eindhoven, 2011.